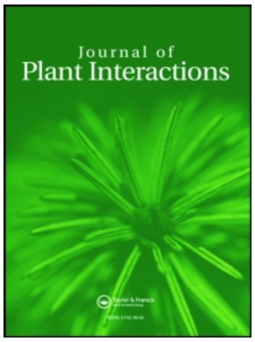

Journal of Plant Interactions

ISSN: 1742-9145 (Print) 1742-9153 (Online) Journal homepage: https://www.tandfonline.com/loi/tjpi20

Leaf stiffness of two Moraceae species based on leaf tensity determined by compressing different external gripping forces under dehydration stress

Deke Xing, Xiaole Chen, Yanyou Wu, Qian Chen, Lin Li, Weiguo Fu & Yu Shu

To cite this article: Deke Xing, Xiaole Chen, Yanyou Wu, Qian Chen, Lin Li, Weiguo Fu & Yu Shu (2019) Leaf stiffness of two Moraceae species based on leaf tensity determined by compressing different external gripping forces under dehydration stress, Journal of Plant Interactions, 14:1, 610-616, DOI: 10.1080/17429145.2019.1686182

To link to this article: https://doi.org/10.1080/17429145.2019.1686182

JOURNAL OF PLANT INTERACTIONS
2019, VOL. 14, NO. 1, 610–616
https://doi.org/10.1080/17429145.2019.1686182

Taylor & Francis
Taylor & Francis Group

Leaf stiffness of two Moraceae species based on leaf tensity determined by compressing different external gripping forces under dehydration stress

Deke Xing[a], Xiaole Chen[a], Yanyou Wu[b], Qian Chen[a], Lin Li[a], Weiguo Fu[a] and Yu Shu[a]

[a]Key Laboratory of Modern Agricultural Equipment and Technology, Ministry of Education, Institute of Agricultural Engineering, Jiangsu University, Zhenjiang, People's Republic of China; [b]Research Center for Environmental Bio-Science and Technology, State Key Laboratory of Environmental Geochemistry, Chinese Academy of Sciences, Institute of Geochemistry, Guiyang, People's Republic of China

ABSTRACT
Leaf water status determination based on mechanical and electrophysiological properties helps determine the inherent as well as instantaneous leaf dehydration tolerance synchronously. The leaf water potential (Ψ_L), physiological capacitance (CP) and gripping force (*F*) were determined with leaves of *Broussonetia papyrifera* (L.) Vent. and *Morus alba* L. Real-time leaf stiffness (LCS_{rt}) and maximum leaf stiffness (LCS_{max}) were investigated by compressing a leaf with external gripping force. Results indicated that LT displayed good correlation with *F*. Compared to *M. alba*, a better instantaneous dehydration tolerance or pressure resistance in *B. papyrifera* was correlated to its persistent stronger LCS_{rt} or LCS_{max}, respectively. *B. papyrifera* showed better flexibility and tolerance to wider range of pressure than *M. alba*. The higher leaf mechanical strength helped to maintain a higher outward pulling force of cell walls; thus, the subsequent negative pressure effectively inhibited cellular water loss. *B. papyrifera* exhibited better drought resistance than *M. alba*.

ARTICLE HISTORY
Received 30 August 2019
Accepted 1 October 2019

KEYWORDS
Leaf stiffness; leaf tensity; pressure resistance; cellular water loss; drought resistance

Introduction

Water maintains cell tension and helps branches and leaves stand upright. Furthermore, it generates turgor that contributes to the movement of stoma or other plant structures and cellular growth (Kroeger et al. 2011). Plant growth is often affected by biotic or abiotic stresses, one of which is drought (Grossi et al. 2016). However, drought resistance differs amongst plant species, and the rapid determination of plant drought resistance helps in the implementation of appropriate irrigation strategies on the plant (Egea et al. 2017). The assessment of leaf traits is one of the methods for studying plant drought resistance (Petrov et al. 2018), a slower water loss rate in the leaf is associated with better drought resistance of plants (Zhou et al. 2018).

Leaf water status could be rapidly determined by analyzing the variation of leaf tensity (LT) during the water loss process (Zhang et al. 2015). Calculated according to the coupling relationship between leaf water potential (Ψ_L) and physiological capacitance (CP), LT reflected water status better than Ψ_L, and Ψ_L was easily affected by the environment (Javed et al. 2017). The online monitoring and prediction of leaf water status can be realized through the determination of LT. However, pressure variation caused by the gripping force (which was used for clamping leaf during the CP determination) changes the concentration of the cytosol solute and the elasticity and plasticity of the cells in the leaf, which causes dielectric constant variation in the cytosol solute. Thus, the values of LT change (Zhang et al. 2015). Therefore, the subsequently assessed plant drought resistance varies as gripping force changes. As such, the plant drought resistance determined by using a specific gripping force was defined as instantaneous drought resistance. Measurements of CP should be conducted under the same gripping force, in order to make the comparison of drought resistance among different plant species credible. However, it is difficult to keep the gripping force consistent at each measurement (Xing et al. 2018). Therefore, it is unreasonable to compare the drought resistance among different plant species only based on the electrophysiological properties.

Mechanical properties, which are closely related to the internal architectures, proved to be another useful tool to investigate drought resistance of plants (Balsamo et al. 2015). Leaf mechanical properties were affected by water status, and a positive correlation between leaf internal architecture, tensile strength and tolerance to dehydration for grasses were observed (Balsamo et al. 2006; Rascio et al. 2015). Plant cells are composed of the cell wall and intracavitary substances (mainly protoplasm), and cell turgor plays an important role in the mechanical stability (Malgat et al. 2016). The wall, located outside the membrane, is a thick and tough layer with a slight elasticity. It not only forms a strong network that functions like a boundary, preventing unconstrained flow of water or nutrition and maintaining internal pressures of cells but also plays key roles in bearing external load and maintaining the mechanical strength of the plant body (Cosgrove 2016). Lignin, which fills in the cellulose cytoskeleton, is a necessary element for the cell walls of all vascular plants. Lignin strengthens the hardness of the cell walls and enhances the mechanical support and compressive strength of the cells (Boerjan et al. 2003). Generally, plants with higher drought resistance could enhance the mechanical strength of cell

CONTACT Deke Xing xingdeke@ujs.edu.cn Key Laboratory of Modern Agricultural Equipment and Technology, Ministry of Education, Institute of Agricultural Engineering, Jiangsu University, Zhenjiang 212013, People's Republic of China; Yanyou Wu wuyanyou@mail.gyig.ac.cn Research Center for Environmental Bio-Science and Technology, State Key Laboratory of Environmental Geochemistry, Institute of Geochemistry, Chinese Academy of Sciences, Guiyang 550081, People's Republic of China

walls by rapidly improving lignin biosynthesis under drought stress conditions (Fan et al. 2006; Yin et al. 2017). High stiffness is correlated to higher mechanical strength of the wall, which subsequently yields negative pressure and effectively inhibits water loss (Deng and Zhang 1998; Charrier et al. 2016). However, mechanical properties are always measured at the point of failure load. Therefore, tissue water status determined based on mechanical properties is an inherent value and implies the inherent drought resistance of plants. Nevertheless, the plant tissues will be damaged irreversibly during the measurement. Therefore, it is hard to continuously monitor plant drought resistance through mechanical properties.

Considering the above drawbacks, the aims of this study were to investigate the coupling relationship between the gripping force and electrophysiological parameters, synchronously determine and assess the inherent and instantaneous plant drought resistances, and combine with the variability of their difference, then comprehensively compare the drought resistance among different plant species. As such, the continuous monitoring of drought resistance of plants can be realized and the influence of inconsistent gripping force on leaf water determining can be reduced or avoided.

Broussonetia papyrifera (L.) Vent. and *Morus alba* L., which belong to the Moraceae family, are characterized by a rapid growth rate and greater adaptability to adversities than other members of the family (Wu et al. 2009). These species are always cultivated as medicinal or ornamental plants. Researches revealed that *B. papyrifera* exhibited better drought resistance than *M. alba* due to its higher bicarbonate use capacity and better water status (Wu and Xing 2012). The latter maintained the LT of *B. papyrifera* (Zhang et al. 2015). In this study, *B. papyrifera* and *M. alba* were selected as experimental materials, researches on the behaviors of leaf mechanical combined with electrophysiological properties under dehydration stress help understand the biomechanics mechanisms of plants in adapting to drought adversity. And a method for rapidly and comprehensively determining plant drought resistance based on the mechanical and electrophysiological properties could be developed.

Materials and methods

Plant materials

The experiment was performed on the campus of Jiangsu University, Jiangsu Province, China (32.20°N, 119.45°E). Eight years old *B. papyrifera* and *M. alba* plants which grew in the yellow-brown soil on a sunny slope were selected as the experimental materials. The area receives a mean annual precipitation of approximate 1100 mm and has a mean annual air temperature of about 15.6°C. Fresh branches from the two plants were picked in July. Leaves growing uniformly were taken from the fourth and fifth leaf positions of each branch. The fresh leaves removed from the branches were placed in double distilled water immediately and soaked for 30 min in order to keep all the leaves in the same initial state (water-saturated), which could make the comparison of drought resistance among different plant species credible. After soaking, water on the surface of the leaves was removed. Finally, the detached leaves were placed on a dry ventilated desktop in the laboratory for 5 h, the temperature was 26°C, Photosynthetic Photon Flux Density (PPFD) was 160 μmol m^{-2} s^{-1}, and relative air humidity was 40%. Measurements were done in triplicate at 0 (baseline), 1, 2, 3, 4 and 5 h after water loss.

Methods

Physical model of LT and F

The gravity equation is:

$$\mathrm{F} = (M_i + m)g \tag{1}$$

where F is the gravity (gripping force; unit: N), M_i is the mass of iron (unit: kg), m is the mass of the foam board and electrode (unit: kg), and g is the acceleration of gravity with a value of 9.80 N kg^{-1}.

Cytosol solute in the leaf was taken as the dielectric. The leaf was clipped between the two electrodes of the parallel-plate capacitor, which formed a parallel-plate capacitor sensor. LT of the plant under different F could be determined by changing the mass of iron in the parallel-plate capacitor (Figure 1(a)). Pressure variation changed the concentration of the cytosol solute and the elasticity and plasticity of the cells in the leaf, which caused dielectric constant variation in the cytosol solute and leaf effective thickness (d_L) between the two electrodes of the parallel-plate capacitor. Thus, the LT changed.

The elasticity of the cell in the leaf was correlated to the water content in the cells. LT differed with plant species under the special F.

The equation for Gibbs's free energy is:

$$\Delta G = \Delta H + PV \tag{2}$$

The equation for the energy of the capacitor is:

$$W_C = \frac{1}{2}U^2CP \tag{3}$$

where W_C is the energy of the capacitor, which is equal to the work converted from Gibbs's free energy (ΔG, $W_C = \Delta G$); ΔH is the internal energy of the system composed of cells in the plant leaves; P is the pressure imposed on the plant cells, V is the volume of plant cells; and U is the test voltage.

P can be calculated using the following equation:

$$P = \frac{F}{A_{CP}} \tag{4}$$

The CP of the leaf was expressed using Equation (5):

$$CP = \frac{\varepsilon_0 \varepsilon_r A_{CP}}{d_L} \tag{5}$$

where ε_0 is the vacuum dielectric constant with a value of 8.854×10^{-12} F m^{-1} and ε_r is the relative dielectric constant of the cytosol solute.

LT was calculated according to Equation (6). The unit was cm^2 cm^{-1} (Zhang et al. 2015):

$$\mathrm{LT} = \frac{A_{\mathrm{CP}}}{d_{\mathrm{L}}} = \frac{CP}{\varepsilon_0}\left[\frac{1000iRT}{81000iRT + (81 - a)M\Psi_{\mathrm{L}}}\right] \tag{6}$$

where A_{CP} is the effective area of the leaf in contact with the capacitor plates (unit: cm^2); d_{L} is the leaf effective thickness (unit: cm); i is the dissociation coefficient (with value of 1); R is the gas constant (with value of 8.30×10^{-3} L MPa mol^{-1} K^{-1}); T is the thermodynamic temperature ($T = 273 + t$°C,

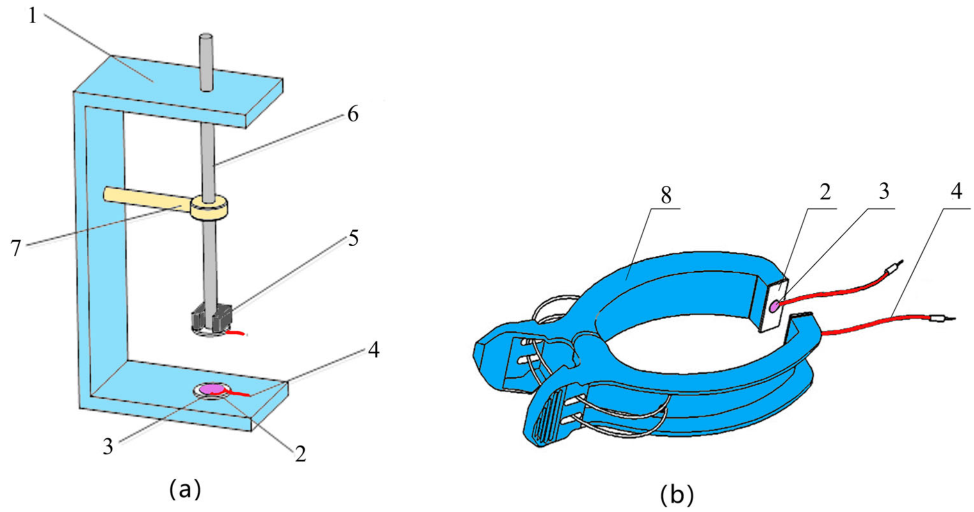

Figure 1. Schematic of the parallel-plate capacitor (a) and (b): 1 = bracket; 2 = foam board; 3 = electrode; 4 = wire; 5 = iron; 6 = plastic bar; 7 = fixation clamp; 8 = plastic clip.

unit: K); ε_0 is the vacuum dielectric constant (with value of 8.854×10^{-12} F m^{-1}); a is the relative dielectric constant of the cytosol solute; M is the relative molecular mass of the cytosol solute (unit: g mol^{-1}); and 81 is the relative dielectric constant of water at normal temperature. In this study, the sugar $C_{12}H_{22}O_{11}$ was identified as the solute in the cytosol; therefore, a was 3.30, M was 342 g mol^{-1}, and t was 20°C. Equation (6) could be rewritten as:

$$\mathrm{LT} = \frac{A_{\mathrm{CP}}}{d_{\mathrm{L}}} = \frac{CP}{717.17 + 96.75\Psi_{\mathrm{L}}} \tag{7}$$

According to Equations (2), (3), (4), (5) and (7), the relationship between LT and F could be expressed as follows:

$$LT = \frac{2\Delta H}{\varepsilon_0 \varepsilon_r U^2} + \frac{2V}{\varepsilon_0 \varepsilon_r A_{CP} U^2} F \tag{8}$$

Incorporating $\frac{2\Delta H}{\varepsilon_0 \varepsilon_r U^2} = y_0$ and $\frac{2V}{\varepsilon_0 \varepsilon_r A_{CP} U^2} = k$ into Equation (8) changes this equation to:

$$LT = y_0 + kF \tag{9}$$

where y_0 and k are the model parameters.

Determination of LT under different F was conducted on fresh leaves taken from fresh branches. The CP of these leaves was measured using an LCR tester (model 3532-50, Hioki, Nagano, Japan). The frequency and voltage used were 3 kHz and 1 V, respectively. Each leaf was clipped onto the custom-made parallel-plate capacitor (a) with a diameter of 10 mm (Figure 1(a)). With a dew point microvoltmeter in a universal sample room (C-52-SF, Psypro, Wescor, Logan, Utah), Ψ_L was measured at the same position of the leaves with the above CP testing.

The relationship curve between LT and F for *B. papyrifera* or *M. alba* was established using Sigmaplot (ver. 12.5, Systat Software, Inc., San Jose, Cal.). The relationship between LT and F was fitted, respectively. The model parameters y_0 and k of *B. papyrifera* or *M. alba* were estimated, respectively.

Calculation of leaf stiffness

The effective thickness per leaf area (d_{LA}, cm cm^{-2}) could be calculated using Equation (10):

$$d_{\mathrm{LA}} = \frac{d_L}{A_{CP}} = 1/\mathrm{LT} \tag{10}$$

During the process where the leaf was compressed by an external force, the moving distance of the force was defined as d_{m} (unit: cm cm^{-2}). According to Equations (9) and (10), d_m could be calculated as follows:

$$d_m = d_{LA0} - d_{LAF} = \frac{kF}{y_0 \times (y_0 + kF)} \tag{11}$$

where d_{LA0} is d_{LA} under 0 N external force and d_{LAF} is d_{LA} under F N external force.

Meanwhile, as the leaf was compressed by an external force, pressure per leaf area was presented as stress (σ, N mm^{-2}). σ was calculated as follows:

$$\sigma = \frac{F}{A_{\mathrm{F}}} \tag{12}$$

where A_{F} is the area of the leaf in contact with the probe implementing the gripping force.

According to Equations (11) and (12), leaf stiffness (LCS) was calculated as follows:

$$\mathrm{LCS} = \frac{\sigma}{d_{\mathrm{m}}} \times 10 = \frac{10 \times y_0 \times (y_0 + kF)}{k \times A_{\mathrm{F}}} \tag{13}$$

The unit of LCS was N mm^{-1}.

Determination of real-time leaf stiffness

LT and F at each moment of water loss were defined as real-time LT ($\mathrm{LT_{rt}}$) and real-time F (F_{rt}), respectively. The CP of leaves at each moment of water loss was measured using the LCR tester with a frequency and voltage of 3 kHz and 1 V, respectively. The leaf was clipped onto the custom-made parallel-plate capacitor (b) with a diameter of 10 mm (Figure 1(b)). With the same dew point microvoltmeter in a universal sample room, Ψ_{L} was also measured at the same position of the leaves with the above CP testing. $\mathrm{LT_{rt}}$ was calculated according to Equation (7) based on the above values of CP and Ψ_{L}, and $\mathrm{F_{rt}}$ was calculated according to Equation (9).

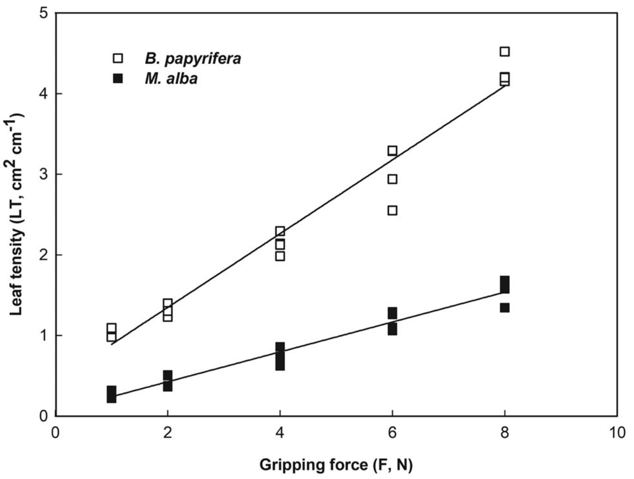

Figure 2. The relationship curve between LT and *F* for *B. papyrifera* or *M. alba*.

The diameter of the probe implementing F_{rt} was 10 mm. A_F was calculated as follows: $A_F = 25\pi$, where the value of π was 3.14. Then LCS_{rt} was calculated by using the following equations: $LCS_{rt} = \frac{10 \times y_0 \times (y_0 + kF_{rt})}{k \times 25\pi}$.

Determination of maximum leaf stiffness

The maximum gripping force (F_{max}) of leaf at each moment of water loss was measured with the texture analyzer TA.XT-Plus (Stable Micro System, United Kingdom) using the P/2n probe with a diameter of 2 mm. The instrument working parameters were determined by the test mode compression; with pretest speed at 2 mm s^{-1}, test speed at 1 mm s^{-1}, post-test speed at 2 mm s^{-1} and trigger force at 100 N (ensure that the leaf is crushed and the cell is broken up).

The diameter of the probe implementing F_{max} was 2 mm, A_F was calculated as follows: $A_F = \pi$, where the value of π was 3.14. Then LCS_{max} was calculated by using the following equations: $LCS_{max} = \frac{10 \times y_0 \times (y_0 + kF_{max})}{k \times \pi}$.

Statistical analysis

All collected data were analyzed using SPSS software (version 13.0, SPSS Inc., New York). The differences between the stress levels were assessed using the least significant difference post-hoc test at 5% significance level ($P \leq .05$). The data were shown as the means ± standard errors determined using the one-sample *T*-test. The confidence interval was 95%.

Results

Relationship between LT and F

The model parameters y_0 and *k* of *B. papyrifera* and *M. alba* were estimated using Equation (9). The relationship curves (Figure 2) between LT and *F* for *B. papyrifera* and *M. alba* was obtained using Sigmaplot (ver. 12.5, Systat Software, Inc., San Jose, Cal.). The relationship between LT and *F* was fitted. The fitting equations between LT and *F* for *B. papyrifera* and *M. alba* were $LT = 0.43 + 0.46F$ ($R^2 = 0.97$, $P < .0001$, $n = 16$) and $LT = 0.06 + 0.19F$ ($R^2 = 0.96$, $P < .0001$, $n = 16$), respectively. Higher *F* values were correlated with higher LT values of *B. papyrifera* and *M. alba*.

Table 1. Leaf water potential (Ψ_L, MPa) and real-time leaf tensity (LT_{rt}, cm^2 cm^{-1}) of *B. papyrifera* and *M. alba*.

	Ψ_L (MPa)		LT_{rt} (cm^2 cm^{-1})	
Time (h)	*B. papyrifera*	*M. alba*	*B. papyrifera*	*M. alba*
0	−1.12 ± 0.03ab	−1.06 ± 0.03a	1.26 ± 0.01a	0.44 ± 0.04a
1	−0.94 ± 0.07a	−1.49 ± 0.10b	1.22 ± 0.11a	0.32 ± 0.02b
2	−1.40 ± 0.11b	−1.73 ± 0.08b	1.14 ± 0.08ab	0.31 ± 0.02b
3	−1.48 ± 0.18b	−2.57 ± 0.13c	0.98 ± 0.01b	0.27 ± 0.01b
4	−2.32 ± 0.11c	−2.81 ± 0.08c	0.81 ± 0.11b	0.20 ± 0.03c
5	−2.78 ± 0.06d	−3.18 ± 0.10d	0.51 ± 0.02c	0.13 ± 0.01d

Note: The mean ± SE ($n = 5$) followed by different letters in the same column differ significantly at $P \leq .05$, according to one-way ANOVA and *t* test.

Ψ_l and LT_{rt} at each moment of water loss

Leaf water potential of *B. papyrifera* was the highest at 1 h and the lowest at 5 h (Table 1). Ψ_L values of *B. papyrifera* at 0, 2 and 3 h exhibited no significant difference. Ψ_L of *M. alba* decreased significantly under drought conditions compared with that at 0 h. The value of Ψ_L at 5 h was the lowest. Values of Ψ_L in *M. alba* at 1 and 2 h or 3 and 4 h exhibited no significant difference. LT_{rt} of *B. papyrifera* at 0, 1 and 2 h showed no significant difference. The LT_{rt} values at 0 and 1 h were the highest, whereas the value at 5 h was the lowest. LT_{rt} of *M. alba* at 0 h was the highest. Low LT_{rt} values were correlated with increasing water loss moments. LT_{rt} values at 1, 2 and 3 h exhibited no significant difference, whereas the value at 5 h was the lowest.

Real-time leaf stiffness

Table 2 shows the values of F_{rt} and LCS_{rt} at each moment of water loss. F_{rt} exhibited the same variation with LT_{rt} within the same plant species. LCS_{rt} of *B. papyrifera* at 1 and 2 h showed no significant difference compared with that at 0 h. These values were higher than those at other water loss moments, and the value at 5 h was the lowest. Low values of LCS_{rt} in *M. alba* were correlated with increasing water loss moment, and the values at 1, 2 and 3 h exhibited no significant difference. Value of LCS_{rt} in *B. papyrifera* at 3 h was still 78% of that at 0 h, while the value of LCS_{rt} in *M. alba* at 1 h decreased to 72% of that at 0 h. Values of LCS_{rt} in *B. papyrifera* were significantly higher than that in *M. alba* at each water loss moment.

Table 2. Real-time gripping force (F_{rt}, N) and real-time leaf stiffness (LCS_{rt}, N mm^{-1}) of *B. papyrifera* and *M. alba*.

	B. papyrifera			*M. alba*		
Time (h)	F_{rt} (N)	LCS_{rt} (N mm^{-1})	[%][a]	F_{rt} (N)	LCS_{rt} ($\times 10^{-1}$ N mm^{-1})	[%][a]
0	1.81 ± 0.02a	0.31 ± 0.01a	100	2.02 ± 0.19a	0.06 ± 0.01a	100
1	1.71 ± 0.24a	0.30 ± 0.03a	96	1.37 ± 0.10b	0.05 ± 0.01b	72
2	1.54 ± 0.17ab	0.28 ± 0.02a	90	1.30 ± 0.10b	0.04 ± 0.01b	69
3	1.21 ± 0.03b	0.25 ± 0.01b	78	1.12 ± 0.02b	0.04 ± 0.00b	62
4	0.83 ± 0.25b	0.20 ± 0.03b	64	0.76 ± 0.15c	0.03 ± 0.01c	46
5	0.16 ± 0.04c	0.13 ± 0.01c	40	0.35 ± 0.04d	0.02 ± 0.00d	28

Notes: The mean ± SE ($n = 5$) followed by different letters in the same column differ significantly at $P \leq .05$, according to one-way ANOVA and t test.
[a] This column stands for the percent value after water loss treatment with reference to that of the 0 h.

Table 3. Maximum gripping force (F_{max}, N) and maximum leaf stiffness (LCS$_{max}$, N mm^{-1}) of *B. papyrifera* and *M. alba*.

	B. papyrifera			*M. alba*		
Time (h)	F_{max} (N)	LCS$_{max}$ (N mm^{-1})	[%][a]	F_{max} (N)	LCS$_{max}$ (N mm^{-1})	[%][a]
0	15.89 ± 0.26f	227.12 ± 3.56f	100	19.35 ± 0.29d	37.05 ± 0.55d	100
1	18.54 ± 0.43e	262.90 ± 5.80e	116	21.45 ± 0.45c	41.01 ± 0.85c	111
2	21.05 ± 0.65d	296.88 ± 8.77d	131	23.94 ± 0.64b	45.69 ± 1.21b	123
3	23.35 ± 0.58c	327.85 ± 7.77c	144	24.41 ± 0.57b	46.58 ± 1.08b	126
4	27.17 ± 0.83b	379.43 ± 11.16b	167	25.64 ± 0.52b	48.91 ± 0.98b	132
5	30.01 ± 1.00a	417.82 ± 13.52a	184	29.54 ± 0.84a	56.24 ± 1.59a	152

Notes: The mean ± SE ($n = 5$) followed by different letters in the same column differ significantly at $P \leq .05$, according to one-way ANOVA and t test.

[a] This column stands for the percent value after water loss treatment with reference to that of the 0 h.

Table 4. Difference between LCS$_{rt}$ and LCS$_{max}$ (LCS$_{vc}$, N mm^{-1}) and variability of LCS$_{vc}$ in *B. papyrifera* and *M. alba* at each water loss moment.

	B. papyrifera			*M. alba*		
Time (h)	LCS$_{vc}$ (N mm^{-1})	[%][a]	Variability[b]	LCS$_{vc}$ (N mm^{-1})	[%][a]	Variability[b]
0	226.81	100	40	37.04	100	24
1	262.60	116	24	41.01	111	13
2	296.60	131	9	45.69	123	1
3	327.60	144	4	46.58	126	2
4	379.22	167	27	48.90	132	8
5	417.69	184	44	56.24	152	28

Note: LCS$_{vc}$ represents the difference between real-time leaf stiffness (LCS$_{rt}$) and maximum leaf stiffness (LCS$_{max}$) at each water loss moment.

[a] This column stands for the percent value after water loss treatment with reference to that of the 0 h.

[b] This column stands for the absolute value of the difference between the percent value at each water loss moment and the average of percent values among six water loss moments.

Maximum leaf stiffness

Table 3 shows the values of F_{max} and LCS$_{max}$ at each moment of water loss. High values of F_{max} in *B. papyrifera* and *M. alba* were correlated with increasing water loss moment. The increase in *B. papyrifera* was more significant than that in *M. alba*. F_{max} of *M. alba* at 2, 3 and 4 h exhibited no significant difference. LCS$_{max}$ exhibited the same variation with F_{max} within the same plant species. Value of LCS$_{max}$ in *B. papyrifera* at 2 h was already 131% of that at 0 h, while the value of LCS$_{max}$ in *M. alba* at 4 h increased to 132% of that at 0 h. Values of LCS$_{max}$ in *B. papyrifera* were significantly higher than that in *M. alba* at each water loss moment.

Variability of the difference between LCS$_{rt}$ and LCS$_{max}$

High values of LCS$_{vc}$ in *B. papyrifera* and *M. alba* were correlated with increasing water loss moment (Table 4). The increase in *B. papyrifera* was more significant than that in *M. alba*. *B. papyrifera* exhibited higher average variability of LCS$_{vc}$ (24.67) than *M. alba* (12.67) during the water loss treatment period.

Discussion

The water loss rate can be used to characterize the dehydration resistance of a detached leaf. Water regulation caused by enzymes, such as carbonic anhydrases (CAs, EC 4.2.1.1), changes the leaf water status under drought conditions (Wu and Xing 2012). And it becomes difficult to diagnose the plant water deficit only by using Ψ_L. The decrease of Ψ_L in *B. papyrifera* at each water loss moment was slighter than that in *M. alba*, which indicated that *B. papyrifera* exhibited better water status than *M. alba* under dehydration stress conditions. However, the moderate decrease of Ψ_L in *B. papyrifera* could help improve water absorption capacity and reduce natural water loss in a short time. This result was consistent with the research by Ren et al. (2015) in rice.

LCS$_{rt}$, which was measured mainly based on the determination of electrophysiological parameters, represented the instantaneous water status determined by using a specific gripping force. When the gripping force used for CP determination was far lower than the force of failure load, the variations of LT$_{rt}$ were always correlated to the vacuolar concentration and the elasticity and plasticity of the cells. Water loss in leaves decreased leaf thickness and increased the vacuolar concentration (Figure 3). LT$_{rt}$ and F$_{rt}$ decreased when the leaves suffered continuous water loss. As a result, the calculated values of LCS$_{rt}$ decreased correspondingly. In fact, a slower water loss speed of leaf caused slighter decrease of LT$_{rt}$ in *B. papyrifera* than that in *M. alba*. The LCS$_{rt}$ in *B. papyrifera* decreased by only 22% in the third hours, while the value in *M. alba* decreased by 28% in the first hour. The persistent stronger LCS$_{rt}$ at water loss moment meant better instantaneous dehydration tolerance in *B. papyrifera*. However, some researches have demonstrated that the pressure variation caused by the gripping force also changed the vacuolar concentration, which influenced the LT$_{rt}$. As a result, the subsequently assessed drought resistance varied as gripping force changed (Zhang et al. 2015; Xing et al. 2018). Therefore, it was unreasonable to compare the drought resistance only based on the electrophysiological properties.

LCS$_{max}$, which was measured mainly based on the determination of mechanical parameters, represented the inherent water status. It was closely related to the leaf internal architectures. Plant cells need to maintain the dynamic balance of a variety of forces under adversity. For example, it is necessary to have a certain elasticity so as to stretch the cells, or an appropriate stiffness to maintain turgor (Malgat et al. 2016). Water adversity provokes lignin synthesis and cell-wall thickening (Eynck et al. 2012), which provide mechanical support for the wall and prevents the cell wall from collapsing caused by negative pressure during plant transpiration (Lewis and Yamamoto 1990). At the moment the cell lost water and shrank, the wall with stronger stiffness pulled out the plasma membrane and produced negative pressure. As a result, the continuous water loss in the cell was effectively inhibited, thus decreasing the water loss rate (Deng and Zhang 1998). When the gripping force implemented on leaves was high enough (equal to failure load), leaf cells could no longer shrink, and F_{max} was mainly influenced by the substance composition of leaf cells (Figure 3). Since lignin synthesis and cell wall thickening of plants could be provoked by water deficit, F_{max} increased when the leaves suffered continuous water loss. As a result, the calculated values of LT$_{max}$ and LCS$_{max}$ increased correspondingly. A stronger

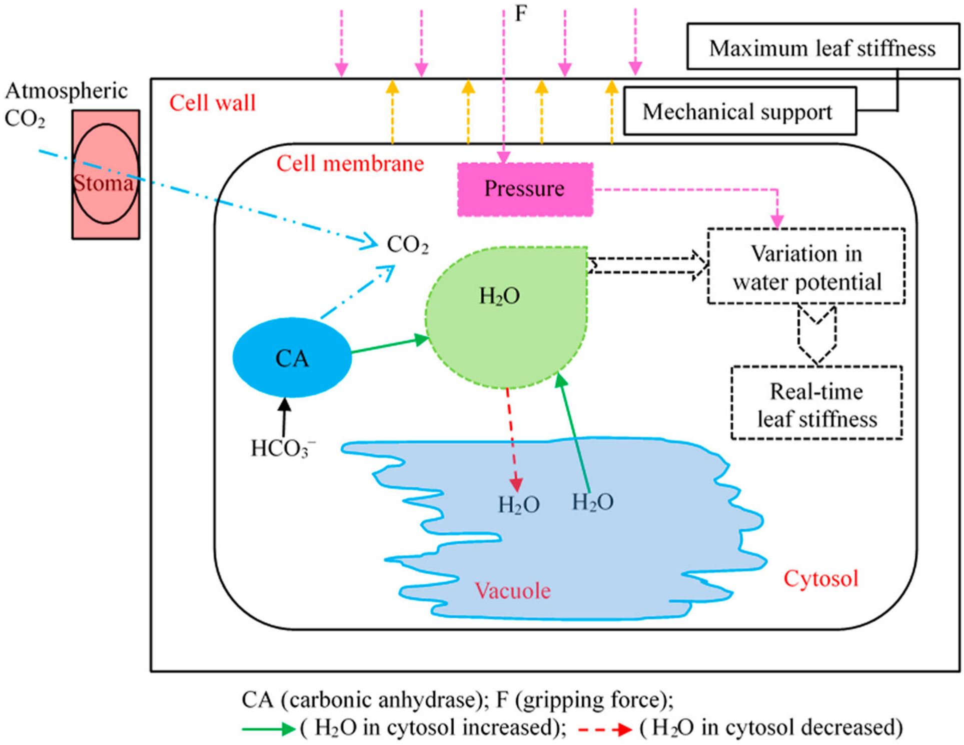

Figure 3. Relationships between water potential, gripping force (*F*) and real-time LCS, maximum LCS.

lignin synthesis and cell-wall thickening capacity in drought-tolerant plants caused more significant increase of LCS_{max} in *B. papyrifera* than that in *M. alba*. Higher LCS_{max} values at each water loss moment and more significant increase of LCS_{max} with increasing water loss time indicated that *B. papyrifera* exhibited better pressure resistance under dehydration conditions. Besides, the above response trait could also be used for evaluating the quality of *B. papyrifera* tissues when they were used as raw materials for paper-making. However, since the LCS_{max} needed to be measured at the point of failure load, the plant tissues would be damaged irreversibly during the determination, therefore, it became hard to realize the online monitoring of plant drought resistance.

The difference between LCS_{max} and LCS_{rt} was defined as leaf stiffness variable capacity (LCS_{vc}) in this study. The average variability of LCS_{vc} during the water loss treatment period could represent the flexibility and range of external forces tolerated by leaf. The average variability of LCS_{vc} in *B. papyrifera* was higher than that in *M. alba*, which indicated that the leaves of *B. papyrifera* showed better flexibility and tolerance to a wider range of external forces under dehydration conditions. The higher leaf mechanical strength in *B. papyrifera* helped to maintain a higher outward pulling force of cell walls in the leaf; thus, the subsequent negative pressure could effectively inhibit cellular water loss. Therefore, *B. papyrifera* exhibited better drought resistance than *M. alba*. This result is consistent with the results of the studies by Wu et al. (2009) and Zhang et al. (2015).

Conclusions

Leaf water potential could not completely reflect the plant water status due to the influences of the surroundings and water regulation caused by enzymes, such as CA in plants. Although the determination of LT was less influenced by the surroundings, the results were easily affected by the area of the leaf in contact with the plates of custom-made parallel-plate capacitor or the gripping force. In this study, the variations of leaf mechanical and electrophysiological properties were synchronously analyzed by determining LT together with *F*; thus, LCS_{rt}, LCS_{max} and the variability of LCS_{vc} were investigated to analyze the leaf dehydration tolerance. The influence caused by the variation of the leaf area in contact with the plates of the custom-made parallel-plate capacitor and inconsistent gripping force could be reduced or avoided.

LT displayed good correlation with *F*. The persistent stronger LCS_{rt}, more significant increase in LCS_{max}, together with the higher average variability of LCS_{vc} indicated that *B. papyrifera* exhibited better pressure resistance and better flexibility and tolerance to wider range of external forces under dehydration conditions. The higher leaf mechanical strength in *B. papyrifera* helped to maintain a higher outward pulling force of cell walls in the leaf; thus, the subsequent negative pressure could effectively inhibit cellular water loss. Therefore, *B. papyrifera* exhibited better drought resistance than *M. alba*. The synchronous investigation of LCS_{rt}, LCS_{max} and the variability of LCS_{vc} could not only realize the online monitoring of plant drought resistance but also reduce the influence of inconsistent gripping force on leaf water determination. The above-mentioned method could also be used for detecting the plant responses to other environmental stresses.

Disclosure statement

No potential conflict of interest was reported by the authors.

Funding

This work was supported by the project of National Key Research and Development Program of China [grant number 2016YFC0502602]; National Natural Science Foundation of China [grant number U1612441, 31301243]; Natural Science Foundation of Jiangsu Province [grant number BK20180863]; and Priority Academic Program Development [PAPD] of Jiangsu Higher Education Institutions.

Notes on contributors

Deke Xing is an Associate Professor in Key Laboratory of Modern Agricultural Equipment and Technology, Ministry of Education, Institute of Agricultural Engineering, Jiangsu University, Zhenjiang, China.

Xiaole Chen is a research assistant, Key Laboratory of Modern Agricultural Equipment and Technology, Ministry of Education, Institute of Agricultural Engineering, Jiangsu University, Zhenjiang, China.

Yanyou Wu is a Professor, Research Center for Environmental Bio-Science and Technology, State Key Laboratory of Environmental Geochemistry, Institute of Geochemistry, Chinese Academy of Sciences, Guiyang, China.

Qian Chen is a research assistant, Key Laboratory of Modern Agricultural Equipment and Technology, Ministry of Education, Institute of Agricultural Engineering, Jiangsu University, Zhenjiang, China.

Lin Li is a research assistant, Key Laboratory of Modern Agricultural Equipment and Technology, Ministry of Education, Institute of Agricultural Engineering, Jiangsu University, Zhenjiang, China.

Weiguo Fu is Professor, Key Laboratory of Modern Agricultural Equipment and Technology, Ministry of Education, Institute of Agricultural Engineering, Jiangsu University, Zhenjiang, China.

Yu Shu is a research assistant, Key Laboratory of Modern Agricultural Equipment and Technology, Ministry of Education, Institute of Agricultural Engineering, Jiangsu University, Zhenjiang, China.

ORCID

Deke Xing http://orcid.org/0000-0001-5834-4306

References

Balsamo R, Boak M, Nagle K, Peethambaran B, Layton B. 2015. Leaf biomechanical properties in *Arabidopsis thaliana* polysaccharide mutants affect drought survival. J Biomech. 48(15):4124–4129. DOI:10.1016/j.jbiomech.2015.10.016

Balsamo RA, Willigen CV, Bauer AM, Farrant J. 2006. Drought tolerance of selected *Eragrostis* species correlates with leaf tensile properties. Ann Bot. 97:985–991. DOI:10.1093/aob/mcl068

Boerjan W, Ralph J, Baucher M. 2003. Lignin biosynthesis. Annu Rev Plant Biol. 54:519–546. DOI:10.1146/annurev.arplant.54.031902.134938

Charrier G, Torres-Ruiz JM, Badel E, Burlett R, Choat B, Cochard H, Delmas CEL, Domec JC, Jansen S, King A, et al. 2016. Evidence for hydraulic vulnerability segmentation and lack of xylem refilling under tension. Plant Physiol. 172(3):1657–1668. DOI:10.1104/pp.16.01079

Cosgrove DJ. 2016. Plant cell wall extensibility: connecting plant cell growth with cell wall structure, mechanics, and the action of wall-modifying enzymes. J Exp Bot. 67(2):463–476. DOI:10.1093/jxb/erv511

Deng WS, Zhang DP. 1998. Water relation-related mechanism of the changes in the sensibility of the growth of grape berry to drought during the berry development. Acta Hortic Sin. 25(2):123–128. In Chinese. http://www.cqvip.com/read/read.aspx?id=3030441

Egea G, Fernández JE, Alcon F. 2017. Financial assessment of adopting irrigation technology for plant-based regulated deficit irrigation scheduling in super high-density olive orchards. Agr Water Manage. 187:47–56. DOI:10.1016/j.agwat.2017.03.008

Eynck C, Séguin-Swartz G, Clarke WE, Parkin IAP. 2012. Monolignol biosynthesis is associated with resistance to *Sclerotinia sclerotiorum* in *Camelina sativa*. Mol Plant Pathol. 13:887–899. DOI:10.1111/j.1364-3703.2012.00798.x

Fan L, Linker R, Gepstein S, Tanimoto E, Yamamoto R, Neumann PM. 2006. Progressive inhibition by water deficit of cell wall extensibility and growth along the elongation zone of maize roots is related to increased lignin metabolism and progressive stelar accumulation of wall phenolics. Plant Physiol. 140(2):603–612. DOI:10.1104/pp.105.073130

Grossi D, Rustioni L, Lorenzo GSD, Failla O, Brancadoro L. 2016. Water deficit effects on grapevine woody tissue pigmentations. Hortic Sci. 43:188–194. DOI:10.17221/186/2015-HORTSCI

Javed Q, Wu YY, Azeem A, Ullah I. 2017. Evaluation of irrigation effects using diluted salted water based on electrophysiological properties of plants. J Plant Interact. 12(1):219–227. DOI:10.1080/17429145.2017.1319501

Kroeger JH, Zerzour R, Geitmann A. 2011. Regulator or driving force? The role of turgor pressure in oscillatory plant cell growth. PLOS ONE. 6(4):e18549. DOI:10.1371/journal.pone.0018549

Lewis NG, Yamamoto E. 1990. Lignin: occurrence, biogenesis and biodegradation. Ann Rev Plant Physiol Plant Mol Biol. 41(1):455–496. DOI:10.1146/annurev.arplant.41.1.455

Malgat R, Faure F, Boudaoud A. 2016. A mechanical model to interpret cell-scale indentation experiments on plant tissues in terms of cell wall elasticity and turgor pressure. Front Plant Sci. 7:1–11. DOI:10.3389/fpls.2016.01351

Petrov P, Petrova A, Dimitrov I, Tashev T, Olsovska K, Brestic M, Misheva S. 2018. Relationships between leaf morpho-anatomy, water status and cell membrane stability in leaves of wheat seedlings subjected to severe soil drought. J Agron Crop Sci. 204(3):219–227. DOI:10.1111/jac.12255

Rascio A, Rascio N, Rinaldi M, Valentini M. 2015. Functional, histological and biomechanical characterization of wheat water-mutant leaves. Physiol Plantarum. 154(2):210–222. DOI:10.1111/ppl.12280

Ren BB, Wang M, Chen YP, Sun GM, Li Y, Shen QR, Guo SW. 2015. Water absorption is affected by the nitrogen supply to rice plants. Plant Soil. 396(1–2):397–410. DOI:10.1007/s11104-015-2603-5

Wu YY, Liu CQ, Li PP, Wang JZ, Xing DK, Wang BL. 2009. Photosynthetic characteristics involved in adaptability to Karst soil and alien invasion of paper mulberry (*Broussonetia papyrifera* (L.) vent.) in comparison with mulberry (*Morus alba* L.). Photosynthetica. 47(1):155–160. DOI:10.1007/s11099-009-0026-3

Wu YY, Xing DK. 2012. Effect of bicarbonate treatment on photosynthetic assimilation of inorganic carbon in two plant species of Moraceae. Photosynthetica. 50(4):587–594. DOI:10.1007/s11099-012-0065-z

Xing DK, Xu XJ, Wu YY, Liu YJ, Wu YS, Ni JH, Azeem A. 2018. Leaf tensity: a method for rapid determination of water requirement information in *Brassica napus* L. J Plant Interact. 13(1):380–387. DOI:10.1080/17429145.2018.1478006

Yin NW, Li JN, Liu X, Lian JP, Fu C, Li W, Jiang JY, Xue YF, Wang J, Chai YR. 2017. Lignification response and the difference between stem and root of *Brassica napus* under heat and drought compound stress. Acta Agron Sin. 43(11):1689–1695. In Chinese. DOI:10.3724/SP.J.1006.2017.01689

Zhang MM, Wu YY, Xing DK, Zhao K, Yu R. 2015. Rapid measurement of drought resistance in plants based on electrophysiological properties. T ASABE. 58(6):1441–1446. DOI:10.13031/trans.58.11022

Zhou AM, Liu EH, Liu J, Feng S, Gong SF, Wang JG. 2018. Characterization of increased cuticular wax mutant and analysis of genes involved in wax biosynthesis in *Dianthus spiculifolius*. Hortic Res. 5:1–9. DOI:10.1038/s41438-018-0044-z